

Several results on the finite-size corrections in the Sherrington–Kirkpatrick spin-glass model

G Parisi†, F Ritort†† and F Slanina§

† Dipartimento di Fisica, Università di Roma II, 'Tor Vergata', and INFN, Sezione di Roma, 'Tor Vergata', Via della Ricerca Scientifica, I-00133 Roma, Italy

†† Departament de Física Fonamental, Universitat de Barcelona, Diagonal 648, 08028 Barcelona, Spain

§ INFN, Sezione di Roma, I Università di Roma 'La Sapienza', P.le Aldo Moro 2, I-00185 Roma, Italy and Institute of Physics, Czech Academy of Sciences, Na Slovance 2, CS-18040 Praha, Czechoslovakia

Received 31 July 1992

Abstract. We present several results on the finite-size corrections in the SK model within the spin-glass phase slightly below the transition temperature and along the de Almeida–Thouless (AT) line. In the first case, we study the finite-size corrections for the distribution of overlaps $P(q)$ and for ultrametricity. Along the AT line, finite-size corrections to the free and internal energy are also obtained. Numerical results are in good agreement with our predictions.

1. Introduction

Although the mean-field solution to the Sherrington–Kirkpatrick (SK) model [1, 2] was completed a decade ago [3] and the interpretation of the result followed soon after that [4, 5], some open problems still remain. In the infinite-dimension limit, the solution is known to be marginally stable [6], but it is unknown whether the peculiar ultrametric structure with an infinite number of ground states survives even in the finite-dimensional case [7, 8]. Even though the question is far from being settled some numerical results are available [13]. Similar questions can be asked in the case of fully connected but finite-volume systems. The method which offers itself in both cases is straightforward in principle and is based on the replica field theory (RFT), which is nothing other than the expansion around the mean-field solution. Free propagators of RFT are known [9], but the formulae are still too complicated to permit explicit calculation of diagrams. The complication arises from the presence of infinitely many zero modes in the fluctuation spectrum around the mean-field solution [10]. In cases where only the limiting behaviour of the propagators in some region is required, approximative formulae [11, 12] can be successfully used. We will follow this way here.

Results from the numerical simulations are available [14, 15] which clearly indicate an approach to the quantities of interest to the infinite-volume theoretical predictions, but the theoretical findings about the value of the finite-size corrections itself would substantially strengthen the consequences about the validity of the 'canonical' ultrametric solution of the SK model.

Recently we have studied the problem at the critical temperature [17], where the situation is quite simple because we can explicitly control the divergence of the Gaussian fluctuations when we lower the temperature to the critical point. In this paper we want to look at the

situation below the critical point and to establish which conclusions can be drawn from the known form of the Gaussian propagators for the SK model. Moreover, at the de Almeida-Thouless (AT) line we can proceed similarly as at the critical point, only the computational difficulty increases.

In section 2 we derive the formulae for the finite-size corrections for the distribution of overlaps and for the violation of ultrametricity, starting with the effective Lagrangian of the SK model near the critical temperature. We then proceed in section 3 with the diagrammatic computation of these quantities. The much simpler particular case of the AT line is studied in section 4. Sections 5 and 6 are devoted to some new results from numerical simulations of the finite-size corrections and their comparison with the theoretical predictions of the preceding sections. The final discussion is presented in the closing section.

2. Corrections to the distribution of overlaps and violation of ultrametricity

Near the critical temperature the SK model is described by the effective Lagrangian [18], which is, in the approximation taking only the fourth-order term inducing the replica symmetry breaking [3],

$$\mathcal{L}[q] = \tau \sum_{(\alpha\beta)} q_{(\alpha\beta)}^2 - \frac{1}{6} \sum_{\alpha\beta\gamma} q_{(\alpha\beta)} q_{(\beta\gamma)} q_{(\gamma\alpha)} - \frac{1}{12} \sum_{\alpha\beta} q_{(\alpha\beta)}^4 - \frac{1}{2} h^2 \sum_{\alpha\beta} q_{(\alpha\beta)} \quad (1)$$

where $\tau = 1 - 1/T$. The mean-field solution is described by the function $q(x)$ which corresponds to the average of the field variable $q_{0(\alpha\beta)} = \langle q_{(\alpha\beta)} \rangle$. The Gaussian fluctuations around the saddle point are formally infinite. In order to regularize the theory it is convenient to consider the free propagator $G(p)$ to be defined as

$$(G^{-1})_{\alpha\beta;\gamma\delta} = p^2 + \frac{\partial^2 \mathcal{L}[q_0]}{\partial \varphi_{(\alpha\beta)} \partial \varphi_{(\gamma\delta)}} \quad (2)$$

where $\varphi_{(\alpha\beta)}$ is the fluctuating part of the $q_{(\alpha\beta)}$ order parameter, i.e. $q_{(\alpha\beta)} = q_{0(\alpha\beta)} + \varphi_{(\alpha\beta)}$. The presence of the zero modes [10] causes the divergence of G when we remove the regularization, i.e. for $p \rightarrow 0$. The regularization can be introduced by adding a term $p^2 \sum_{(\alpha\beta)} \varphi_{(\alpha\beta)}$ to the Lagrangian.

Without any zero modes, as in the case of ferromagnetic ordering, the propagators would give us directly the leading term of the finite-size corrections. Here, because of the divergence, we have to sum all the perturbation series (which is the $1/N$ expansion) and send $p \rightarrow 0$ at the end. Supposing that the sum of the perturbation series is finite in the $p \rightarrow 0$ limit, we can deduce the N -dependence of the leading term of the sum. Because of the complexity of the free propagators, it would be very difficult to compute diagrams arising in the $1/N$ expansion. Nevertheless, the $p \rightarrow 0$ behaviour of the propagators can be found and that is sufficient to make some statements about the $p \rightarrow 0$ behaviour of the diagrams.

As it was shown in [17], only the term cubic in the fluctuation $\varphi_{(\alpha\beta)}$ is relevant for the leading term in the finite-size corrections. Hence, equation (1) implies that the effective Lagrangian describing the fluctuations around the mean-field solution is

$$\mathcal{L}_R[\varphi] = \sum_{(\alpha\beta)(\gamma\delta)} \varphi_{(\alpha\beta)} (G^{-1})_{\alpha\beta;\gamma\delta} \varphi_{(\gamma\delta)} - \frac{1}{6} \sum_{\alpha\beta\gamma} \varphi_{(\alpha\beta)} \varphi_{(\beta\gamma)} \varphi_{(\gamma\alpha)} - \frac{1}{3} \sum_{\alpha\beta} q_{0(\alpha\beta)} \varphi_{(\alpha\beta)}^3 \quad (3)$$

By this definition we have incorporated the regularization parameter p directly in the Lagrangian. We will denote the averages with respect to this Lagrangian by angle brackets, keeping in mind that they are functions of p . The diagrams in question contain only two types of cubic vertices.

The quantities of interest will be the distribution of overlaps $P(q)$ and the distributions describing the ultrametricity $P(q_1, q_2, q_3)$ and $\tilde{P}(\delta q)$, defined via their moments

$$M_k = \int dq P(q) q^k = \lim_{n \rightarrow 0} \frac{1}{n(n-1)} \sum_{\alpha\beta} \langle q_{(\alpha\beta)}^k \rangle \quad (4)$$

$$\int dq_1 dq_2 dq_3 P(q_1, q_2, q_3) q_1^{k_1} q_2^{k_2} q_3^{k_3} = \lim_{n \rightarrow 0} \frac{1}{n(n-1)(n-2)} \sum_{\alpha\beta\gamma} \langle q_{(\alpha\beta)}^{k_1} q_{(\beta\gamma)}^{k_2} q_{(\gamma\alpha)}^{k_3} \rangle \quad (5)$$

$$\mu_k = \int d\delta q \tilde{P}(\delta q) (\delta q)^k = \int dq_1 d\delta q dq_2 P(q_1, q_2, q_2 + \delta q) \theta(q_1 - q_2) \theta(q_1 - q_2 - \delta q) (\delta q)^k. \quad (6)$$

The latter functions can be obtained following the procedure applied in [4]. We have found for the distribution of overlaps

$$P(q) = \left(\frac{dq(x)}{dx} \right)^{-1} \left(1 + \langle \varphi_{(\alpha\beta)} \rangle \frac{\partial}{\partial q} + \langle \varphi_{(\alpha\beta)}^2 \rangle \frac{\partial^2}{\partial q^2} + \dots \right). \quad (7)$$

This formula is somewhat formal but we can find a simple interpretation of it.

We define $P_0(q) = 1/(dq(x)/dx)$, the infinite-volume limit, and write

$$P(q) = \int d\bar{q} P_0(\bar{q}) K_{\bar{q}}(q - \bar{q}). \quad (8)$$

We now use the notation introduced in [9]. Because of the ultrametricity property of the Parisi solution we parametrize the Green functions $G_{\alpha\beta;\gamma\delta}$ by $G_{z_1 z_2}^{xy}$. In this notation the superscripts x and y are given by $q(x) = q_{\alpha\beta}$ and $q(y) = q_{\gamma\delta}$. The subscripts z_1 and z_2 are given by $q(z_1) = \max(q_{\alpha\gamma}, q_{\alpha\delta})$ and $q(z_2) = \max(q_{\beta\gamma}, q_{\beta\delta})$ respectively.

Denoting the shift of the order parameter function by $\varphi(x) = \langle \varphi_{(\alpha\beta)} \rangle$ and $\bar{G}_{11}^{xx} = \langle \varphi_{(\alpha\beta)}^2 \rangle$ the diagonal element of the full propagator, we can see that the cumulants of the function $K_{\bar{q}}(q)$ are simply

$$\begin{aligned} C_0 &= 1 \\ C_1 &= \varphi(x(\bar{q})) \\ C_2 &= \bar{G}_{11}^{x(\bar{q})x(\bar{q})} - \varphi^2(x(\bar{q})) \quad \dots \end{aligned} \quad (9)$$

In particular, the finite-size corrections to the δ -function part of the function P_0 , which is the feature most simply accessible by simulations, can be expressed by saying that the centre-of-gravity is shifted by $\varphi(x_1)$ and the δ -function acquires a finite width. The square of the width is the matrix element of the propagator $\bar{G}_{11}^{x_1 x_1}$.

The information about the shape of the distribution $\tilde{P}(\delta q)$ can be obtained similarly. The calculation is simple and gives to the lowest order in φ

$$\begin{aligned} \mu_0 &= \frac{1}{2} + O(\langle \varphi^2 \rangle) \\ \mu_2 &= 2 \int_0^1 dx \int_0^x dy (\bar{G}_{11}^{yy} - \bar{G}_{1x}^{yy}) + O(\langle \varphi^4 \rangle) \dots \end{aligned} \quad (10)$$

(All the odd moments vanish due to the symmetry of the function $\tilde{P}(\delta q)$.)

3. In the spin-glass phase at zero magnetic field

In the preceding section we obtained the expression for the quantities of interest in terms of the full (dressed) propagators. In order to compute them we have to write the perturbation series for them, using the free propagators. Now we recall what is known about the $p \rightarrow 0$ behaviour of the free (Gaussian) propagators [11, 12]:

$$\begin{aligned} G_{z_1 z_2}^{xy} &\simeq p^{-4} g_1(x/p, y/p, z_1/p, z_2/p) \\ G_{z_1 z_2}^{xx_1} &\simeq p^{-3} g_2(x/p, z_1/p, z_2/p) \\ G_{z_1 z_2}^{x_1 x_1} &\simeq p^{-2} g_2(z_1/p, z_2/p) \end{aligned} \quad (11)$$

for both $p \rightarrow 0$ and $x, y, z_1, z_2 \rightarrow 0$. Moreover, the functions g_1, g_2, g_3 are not independent. The following relations were found in [11, 12]

$$\begin{aligned} G_{x_1 x_1}^{xx} - G_{11}^{xx} &\sim p^{-3} \\ G_{x_1 z}^{xx} - G_{1z}^{xx} &\sim p^{-3} \\ G_{x_1 x_1}^{xx} - 2G_{1x_1}^{xx} + G_{11}^{xx} &\sim p^{-2}. \end{aligned} \quad (12)$$

From the latter formulae we want to establish the order of the $p \rightarrow 0$ divergence of various diagrams. Introducing the reduced variables $\xi = x/p, \eta = y/p, \dots$ we obtain integrals which do not contain p explicitly, but the upper bounds go to ∞ when $p \rightarrow 0$. Making the crucial supposition that these integrals are finite, we obtain the following rules for power-counting in the diagrammatic expansion:

1. The factor p^{-4} corresponds to each line representing the free propagator.
2. The factor p corresponds to each summation over free replica index and to each factor $q_{0(\alpha\beta)}$.

These rules enable us to hypothesize about the behaviour of perturbation series when $p \rightarrow 0$. First, by looking at the integrals represented by diagrams we can see that adding one loop means multiplying by a factor which behaves like $1/(Np^6)$, regardless of which of the two vertices is present. Hence, if the first term of the perturbation expansion of the quantity Q behaves like $1/(N^l p^m)$ we have $Q \sim N^{-l} p^{-m} f_Q(N^{-1} p^{-6})$. If we send $p \rightarrow 0$ for fixed N , it suggests behaviour similar to $\sim N^{-l+m/6}$ for the leading term in the finite-size corrections for Q .

Applying this simple consideration to the cumulants of the function $K_{\bar{q}}$ for $\bar{q} = q_{\max}$ we get

$$C_k \sim N^{-k/3} \quad k = 2, 3, \dots \quad (13)$$

The cumulant behaviour implies the following form for the function $K_{q_{\max}}$ defined in equation (8)

$$K_{q_{\max}}(q - q_{\max}) \sim N^{1/3} f(N(q - q_{\max})^3). \quad (14)$$

The most important consequence, in our opinion, is that the square of the width of the 'delta-function part' of the distribution of overlaps should scale like $N^{-2/3}$. This result has also been recently obtained by a different method in which the problem of two coupled replicas was studied [20]. Note that the same N -dependence was found for the internal energy at

the critical point [17]. In fact, at T_c both quantities correspond to the same element \bar{G}_{11}^{xx} of the propagator (independent of x in this case).

The moments of the distribution $\tilde{P}(\delta q)$ require further care. Let us look at the second moment μ_2 . From (12) we see that the integral expression in the first term of the perturbation series is, in fact, using the reduced variables

$$-2(G_{\infty\xi}^{\eta\eta} - G_{\infty\infty}^{\eta\eta}) + p^{-3}g(\eta) \quad (15)$$

and, using the explicit formulae for the free propagators [9], we obtain

$$G_{\infty\xi}^{\eta\eta} - G_{\infty\infty}^{\eta\eta} = \int_{\eta}^{\infty} d\kappa_1 \int_{\xi}^{\infty} d\kappa_2 \frac{1}{(p^2 + (\kappa_1/2)^2 + (\kappa_2/2)^2 - (\xi/2)^2)^3} \sim \frac{1}{p^4} \frac{1}{\xi^4} \quad \xi \gg 1. \quad (16)$$

Hence, power-counting gives $N^{-1}p^{-2}$ behaviour for the first term in the perturbation series, i.e.

$$\mu_2 \sim N^{-2/3}. \quad (17)$$

Unfortunately, we have not found the behaviour for any more quantities. The internal energy behaviour would be particularly desirable. The difficulty stems from the fact that the expression for it contains the sum of several terms. This more complex problem will be discussed in a future work [22].

4. At the de Almeida-Thouless line

The problem of the complicated structure of the propagator is not present on the paramagnetic side of the AT line. The theoretical analysis of the finite-size corrections follows the same arguments as those used at the critical point [17].

The free propagator $G_{\alpha\beta;\gamma\delta}$ has only three independent matrix elements, which can be found explicitly by inverting the Hessian [19] on the paramagnetic side. It is convenient to write the result in the form

$$G_{\alpha\beta;\gamma\delta} = G_1(\delta_{\alpha\gamma}\delta_{\beta\delta} + \delta_{\alpha\delta}\delta_{\beta\gamma}) + G_2(\delta_{\alpha\gamma} + \delta_{\beta\delta} + \delta_{\alpha\delta} + \delta_{\beta\gamma}) + G_3. \quad (18)$$

The full (dressed) propagators will have the same form with three corresponding independent matrix elements $\bar{G}_1, \bar{G}_2, \bar{G}_3$. For completeness we list here the explicit formulae for the free propagator

$$\begin{aligned} G_1 &= \frac{1}{2p^2} & G_2 &= \frac{1}{4p^2} - \frac{1}{2} \frac{1}{2p^2 + 2q_0} \\ G_3 &= \frac{1}{2p^2} - \frac{1}{2p^2 + 2q_0} - \frac{2q_0}{(2p^2 + 2q_0)^2}. \end{aligned} \quad (19)$$

The regularization parameter p is introduced as before because, when approaching the AT line, the propagator will diverge due to the fact that the replicon eigenvalue becomes zero.

Denoting $\bar{\varphi} = \varphi(x)$ and $\bar{G}_D = \bar{G}_{11}^{xx} = \bar{G}_1 + 2\bar{G}_2 + \bar{G}_3$, now independent of x , and performing explicitly the one-loop calculation, we have obtained, for the $p \rightarrow 0$ limit

$$\bar{G}_D = 3(2p^2N)^{-1}(1 + (2p^2)^{-3}N^{-1}(7 - 26q_0 + 44q_0^2) + O(N^{-2}p^{-12})) \quad (20)$$

$$\bar{\varphi} = -3\frac{1-2q_0}{2q_0}(2p^2N)^{-1}(1 + (2p^2)^{-3}N^{-1}(7 - 26q_0 + 44q_0^2) + O(N^{-2}p^{-12})). \quad (21)$$

We can see immediately that both $\bar{G}_D \simeq G_{(-2/3)}N^{-2/3}$ and $\bar{\varphi} \sim N^{-2/3}$. The reason for the coincidence in the exponent is that in the tadpole diagram which is always present in $\bar{\varphi}$ the single connecting line corresponds to the longitudinal eigenvector of the Hessian, which always has a corresponding non-zero eigenvalue.

One important consequence is that the exchange part of the internal energy [17]

$$E_x = \overline{\left\langle -\sum_{i < j} J_{ij} \sigma_i \sigma_j \right\rangle} = -\frac{1}{2T} - \frac{1}{Tn} \sum_{(\alpha\beta)} \left\langle q_{(\alpha\beta)} \left(q_{(\alpha\beta)} - T^2 \frac{\partial \mathcal{L}}{\partial q_{(\alpha\beta)}} \right) \right\rangle \quad n \rightarrow 0 \quad (22)$$

has the following finite-size corrections

$$\delta E_x = \bar{G}_D + 2q_0\bar{\varphi} \sim N^{-2/3}. \quad (23)$$

We see that the leading term of the finite-size corrections is the same as at the critical temperature, but there is a difference in the present case in the source of the next leading term. At the critical temperature it occurred due to the presence of the fourth-order term in the effective Lagrangian. In contrast, here we have a non-zero contribution even from the third-order terms, which suggests that the next-leading contribution to the finite-size corrections will be more significant at the AT line than at the critical temperature.

The leading term of the finite-size corrections for the free energy follows from the above calculations. In fact

$$F = -\frac{T}{Nn} \ln \int \left(\prod_{(\alpha\beta)} \sqrt{N/2\pi T^2} d\varphi_{(\alpha\beta)} \right) \exp \left(-N \left(p^2 \sum_{(\alpha\beta)} \varphi_{(\alpha\beta)} + \mathcal{L}[\varphi] \right) \right). \quad (24)$$

and we find for the derivation of the free energy with respect to p^2

$$\frac{N}{T} \frac{\partial F}{\partial p^2} = \frac{1}{n} \left\langle N \sum_{(\alpha\beta)} \varphi_{(\alpha\beta)}^2 \right\rangle = -\frac{N}{2} \bar{G}_D \quad (25)$$

so that the finite-size corrections δF for the free energy are given by

$$(N/T)\delta F = \ln p^{-2/3} + f(Np^6). \quad (26)$$

In order to have a finite result in the limit $p \rightarrow 0$ the function f should behave like $f(w) \simeq \ln(w^{1/4})$ for $w \rightarrow 0$. Hence,

$$\delta F = T(\ln N/4N) + O(1/N). \quad (27)$$

Note the abrupt change in the leading term of the finite-size corrections from $\ln N/12N$ at the critical point [17] to $\ln N/4N$ at the AT line. This is a manifestation of the change in the

number of zero modes *per replica* from $-1/2$ at the critical point (where all the eigenvalues of the Hessian are zero) to $-3/2$ at the AT line, where only the replicon eigenvalues vanish.

When trying to estimate the finite-size corrections quantitatively, we limit ourselves to \bar{G}_D . We see that it has the form $\bar{G}_D = N^{-2/3} w^{1/3} f(w)$ so that it should be $f(w) \simeq A w^{-1/3}$, $w \rightarrow \infty$. As in [17] we compute an estimate for the coefficient A from the information of the $w \rightarrow 0$ behaviour of the function f . It is nothing other than the analytic continuation from the neighbourhood of the point $w = 0$ to the neighbourhood of $w = \infty$. In [17] we investigated at length the possibilities offered by two methods of doing such a continuation and we will apply the same methods in the present work as well. We say in advance that both of them give the result in the following form

$$G_{(-2/3)}(q_0) = \gamma (1 - \frac{26}{7} q_0 + \frac{44}{7} q_0^2)^{-1/3} \quad (28)$$

and γ depends on the particular procedure used. It means that the temperature dependence of the normalized width of the distribution of overlaps

$$G_{(-2/3)}(q_0)/G_{(-2/3)}(0) \quad (29)$$

is not influenced by the procedure taken and, consequently, numerical measurement of it can test the present theory.

The first method for computing γ is based on the formula

$$f(w) = \sum_{k=0}^{\infty} g(k) (-w)^k = \frac{1}{2i} \int_c dz \frac{g(z)}{\sin \pi z} w^z \simeq -\pi w^s \text{Res} \frac{g(s)}{\sin \pi s} \quad (30)$$

where the last equation holds for $w \rightarrow \infty$ and s is the pole of $g(z)$ with the largest real part. If we know the power-law behaviour of the function $f(w) \simeq A w^s$ at $w \rightarrow \infty$, we can deduce the coefficient A by reasonable choice of the function $g(z)$, fitting the known values of it for several small integers z . In our case we are limited even by the constraint that \bar{G}_D is positive. Trying the function

$$g(z) = ab^z \Gamma(z+1) \cos(\pi z) / (z + \frac{1}{3}) \quad (31)$$

with free parameters a, b , we obtain at the end $\gamma = 0.80637 \dots$

The second procedure consists in simply taking any formula for $f(w)$ which can interpolate between the known $w \rightarrow 0$ and $w \rightarrow \infty$ behaviour. Taking the simplest choice consistent with the requirement $\gamma > 0$, we have $f(w) = ((1 + aw)^2)^{-1/6}$ and we obtain $\gamma = 1.08738 \dots$

As we can see, the results obtained by two independent methods are very close to one to another. This encourages us to claim that these quantitative estimates are near to the correct result. Having only two different estimates it is difficult to reach any firm conclusion, but it at least gives some indication of the exact value. Thus, we finish the section with the following estimate for the coefficient γ

$$\gamma = 0.9 \pm 0.2. \quad (32)$$

5. Numerical results at the AT line

In this section we present the results we have obtained on the study of some quantities at the AT line. We have simulated the SK model with discrete couplings $J = \pm 1/N^{1/2}$.

Along the AT line, the main results concern the nature of the finite-size corrections for the free energy and internal energy. Figure 1 shows the free energy for five different sizes which vary from $N = 32$ up to $N = 256$. These have been obtained by integrating the internal energy from $T = \infty$ down to $T = 0.5$ at constant field $h \simeq 0.57$ (this value of h has been calculated exactly solving the saddle-point equations for the SK model with an applied magnetic field). The number of samples ranges from 1000 to 500 for the largest size. Our results are in reasonable agreement with the theoretical prediction equation (27).

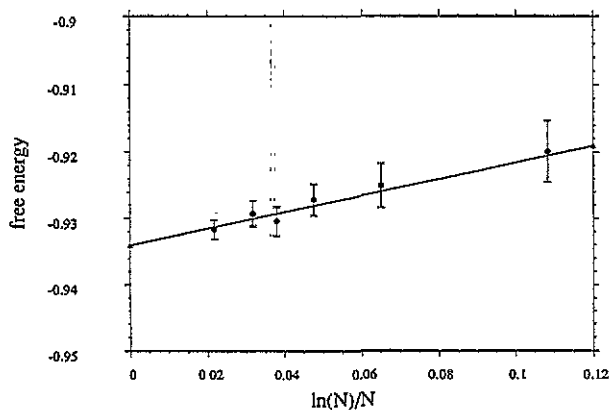


Figure 1. Free energy of the SK model at the AT line ($T = 0.5$, $h \simeq 0.57$). The straight line is the theoretical prediction equation (27).

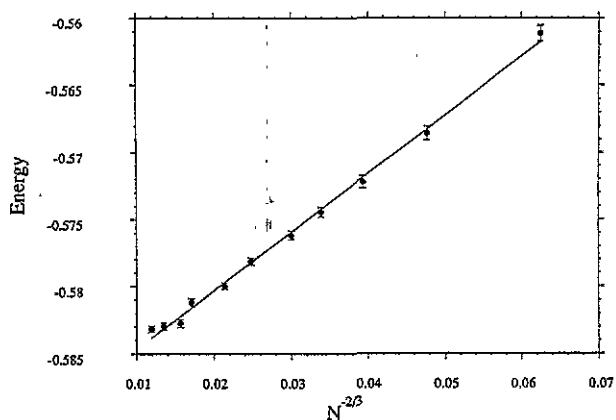


Figure 2. Internal energy E_x from equation (22) at the same point in the AT line as in figure 1. The line is a linear fit to the points using the least squares method and the parameters of the fit are shown in the text.

Figure 2 shows the internal energy at $T = 0.5$, $h \simeq 0.57$. The internal energy is given by two terms:

$$E = \left\langle - \sum_{i < j} J_{ij} \sigma_i \sigma_j - h \sum_{i=1}^N \sigma_i \right\rangle \quad (33)$$

where $\langle \dots \rangle$ is the thermal average and $\overline{(\dots)}$ means average over disorder.

Far from T_c there is an additional finite-size correction which has not been considered in the theoretical derivations. There is a tail for $P(q)$ corresponding to the region of negative overlaps which gives a strong finite-size correction for magnitudes not invariant under the symmetry $\sigma \rightarrow -\sigma$. To avoid this problem we plot in figure 2 the term $\overline{J_{ij} \langle \sigma_i \sigma_j \rangle}$. Twelve sizes ranging from $N = 32$ up to $N = 768$ have been studied and the number of samples varies from 2000 up to 6000 for the lowest sizes. Data are in good agreement with the scaling behaviour equation (23):

$$E_x = E_x(\infty) + a N^{-2/3} \quad (34)$$

and the least-squares fit yields $a \simeq 0.43 (\pm 0.02)$, $U(\infty) = -0.5890 (\pm 5 \times 10^{-4})$ which is very near to the correct result -0.5887 .

One more prediction on the finite-size corrections along the AT line has been tested. This is the variation of the slope in equation (28) near the critical temperature. We have simulated the SK model along the AT line at four temperatures in the (T, h) plane near $T = 1$. Even though finite-size corrections are very sensitive to the critical point we expect the variation of the slope a in equation (34) will reproduce the theoretical behaviour equation (28). The points studied in the AT line are: $(0.8, \simeq 0.117)$, $(0.85, \simeq 7.3 \times 10^{-2})$, $(0.9, \simeq 3.8 \times 10^{-2})$, $(0.95, \simeq 1.3 \times 10^{-2})$. At each point in the AT line, six different sizes $N = 32, 64, 96, 128, 192, 256$ have been simulated with 2000 samples in each case. In order to test the theoretical prediction equation (28) we should calculate the second cumulant of the $P(q)$ in the regime where there is not a tail in the $P(q)$ corresponding to the negative side of the overlaps as was previously commented. Fortunately, near the critical point the order parameter is nearly zero and this effect is negligible (this would not be the case if we were on the AT line far from T_c).

For each point in the h - T plane we make a least-squares fit and we determine the value of b :

$$\langle q^2 \rangle = q_0^2 + b N^{-2/3} \quad (35)$$

where q_0 is the order parameter in the infinite-size limit obtained by solving the saddle-point equations for the SK model with an applied magnetic field. In figure 3 we show the four values obtained for b plotted against q . The different values of b have been fitted with an equation of the type $b = A(1 + Bq_0 + Cq_0^2)^{-1/3}$ and we obtain $A \simeq 1.1$, $B \simeq -3.8$ and $C \simeq 11$. The parameters A and B are in good agreement with the formula in equations (28) and (32). For the value of C there is disagreement. We believe that the reason is the following: in order to obtain b up to second order in q_0 , we should include more terms in the Lagrangian equation (3) but the computation would become much more complex.

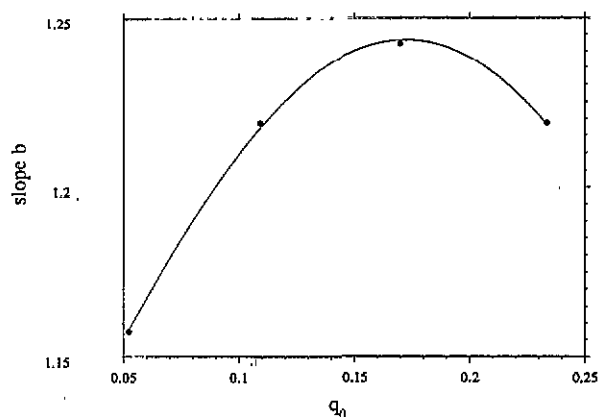


Figure 3. Different values of b in equation (35) at four different points on the AT line near $T_c = 1$ plotted against q_0 . The parameters of the fit are given in the text.

6. Numerical results in the spin-glass phase

Now we comment on the results obtained within the spin-glass phase. We focus on those finite-size corrections which can be easily predicted from the Gaussian propagators. Finite-size corrections for magnitudes like the internal energy will be presented elsewhere. Figure 4 shows the square of the width of the delta-function part of the $P(q)$ in the SK model at $T = 0.8$ and $h = 0$. Eight sizes varying from $N = 64$ up to $N = 640$ have been simulated with a number of samples ranging from 2000 to 500 for the largest sizes. In this case q_{\max} is approximately 0.23 in the infinite size limit. Due to the natural discretization of $P(q)$ for finite sizes we are not able to determine q_{\max} exactly. Then we have calculated the width of the delta-function part taking $q_{\max} = 0.25$ for all sizes which corresponds to the value where $P(q)$, obtained from the simulations, has a maximum.

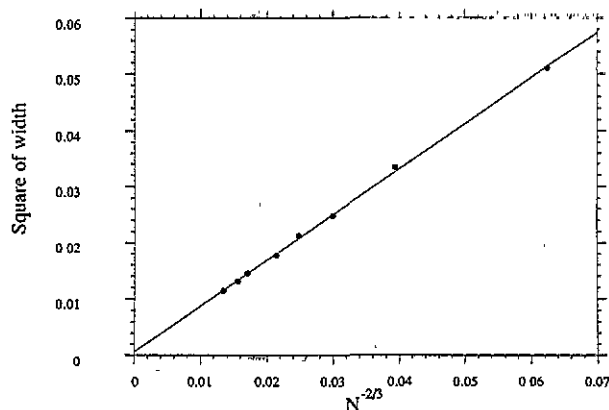


Figure 4. Second cumulant C_2 as defined in equation (9) for the SK model at $T = 0.8$, $h = 0$. The line is a linear fit to the points. It gives $C_2 \approx 0.8 N^{-2/3}$.

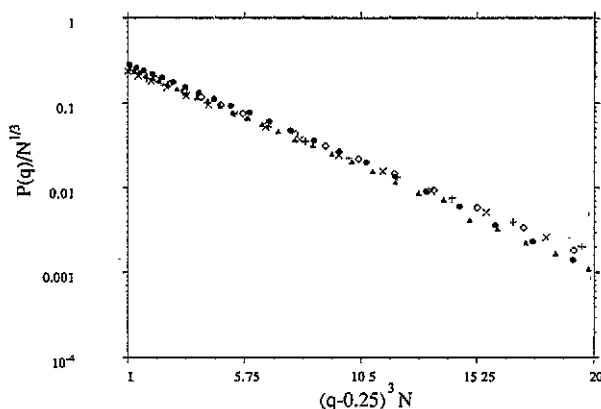


Figure 5. $P(q)/N^{1/3}$ for $q > 0.25$ for the SK model at $T = 0.8$, $h = 0$ plotted against $N(q - 0.25)^3$. The agreement with the scaling law equation (14) is impressive. The symbols are: \bullet , $N = 128$; Δ , $N = 192$; \diamond , $N = 256$; \times , $N = 512$; $+$, $N = 640$.

Figure 5 tests the scaling law equation (14). We plot $P(q)$ when $q > 0.25$ at $T = 0.8$, $h = 0$, for several sizes $N = 128, 192, 256, 512, 640$. All of them fall on the same straight line (of slope $\simeq 0.26$) if the vertical axis has a logarithmic scale. This results implies that

$$P(q > q_{\max}) \sim N^{1/3} \exp(-0.26 N (q - q_{\max})^3) \quad (36)$$

which means that all pure states with an overlap $q_{\alpha\beta}$ outside the support of the function $P(q)$ are thermodynamically unstable. This result and the order of magnitude of the slope (in equation (36)) 0.26 are in agreement with the results in [20].

In addition the prediction, equation (17), has been tested numerically. In this case the hypercube model [16] has been simulated because it is computationally faster than the SK model. The price we pay for fast convergence is that we have finite-size corrections in the SK model which go like $1/D$ or $1/\ln(N)$ since $N = 2^D$. We have simulated the hypercube at $T = 0.7$ and $h = 0$ for eight dimensionalities varying from $D = 6$ up to $D = 13$ (i.e. the sizes range from $N = 64$ up to $N = 8192$) and a number of samples which varies from 1000 up to 24 for case $D = 13$. Figure 6 shows the second moment of $\tilde{P}(\delta q)$ (defined in equation (6)) when q_{\max} lies between 0.1 and 0.3. Given three overlaps $q_{(\alpha\beta)}$, $q_{(\gamma\alpha)}$, $q_{(\beta\gamma)}$, δq is given by the difference between the middle overlap and the smallest one. Our data seem to be in agreement with the predicted behaviour for high dimensionalities (the full line indicates this $N^{-2/3}$ behaviour). It is interesting how strong the finite-dimensionality corrections are in this case (similar effects were found in a previous work [16]).

We have also tried to find some scaling behaviour (like that found for the $P(q)$, see equation (14)) in the case of ultrametricity. According to equation (17) it would not be surprising if the same scaling behaviour were also to be valid in this case. We have simulated the hypercube model at the same dimensions and temperature as before and we have calculated the probability distribution $\tilde{P}(\delta q)$ when the maximum overlap lies between 0.175 and 0.225 since $q_{\max} \simeq 0.36$ and we would like to be far from the region where the pure states are very close (ultrametricity would then be trivial). We have calculated the behaviour $\tilde{P}(\delta q)$ with respect to size for four different values of the overlap difference $\delta q = 0.125, 0.1375, 0.15, 0.1625$. In all four cases, the following scaling law seems to be satisfied (for δq fixed):

$$\tilde{P} \sim \exp(-N g(\delta q)) \quad (37)$$

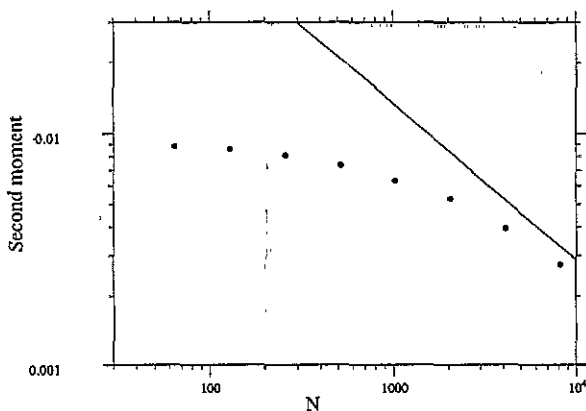


Figure 6. Ultrametricity in the hypercube model at $T = 0.7$ for eight different dimensions from $D = 6$ up to $D = 13$. Even though there are strong finite-dimensional corrections, the data seem to be in agreement with the $N^{-2/3}$ behaviour of equation (17) in the infinite dimension limit (the straight line is $\mu_2 \approx 1.3 N^{-2/3}$ and the value 1.3 is only an estimate).

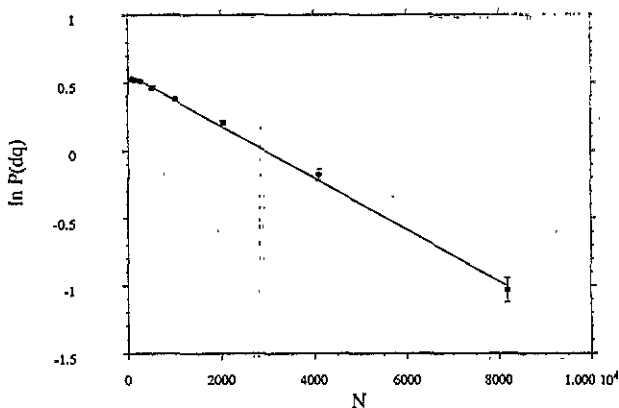


Figure 7. Logarithm of $\tilde{P}(\delta q)$ against size in the hypercube model at $T = 0.7$ for eight different dimensions from $D = 6$ up to $D = 13$. In this case, $\delta q = 0.1625$ and the maximum overlap lies between 0.175 and 0.225.

where $g(\delta q)$ is an unknown function of δq .

Figures 7 and 8 show the logarithm of \tilde{P} against size N at $\delta q = 0.1625$ and $\delta q = 0.125$ respectively. The previous exponential behaviour is in good agreement with the data. It means that ultrametricity is thermodynamically stable and the cost in free energy, when violating it, grows linearly with size [23]. We have also tried to find a scaling law similar to equation (14). There are theoretical arguments which support this result [21]. In this case, we would expect that

$$\tilde{P}(\delta q) = N^{1/3} \exp(a N \delta q^3) \quad (38)$$

where a is a constant.

This means that in equation (37) we take $g(q) \sim q^3$. Figure 9 shows values of $\tilde{P}(\delta q)/N^{1/3}$ for different dimensionalities from $D = 6$ up to $D = 13$ and for four different

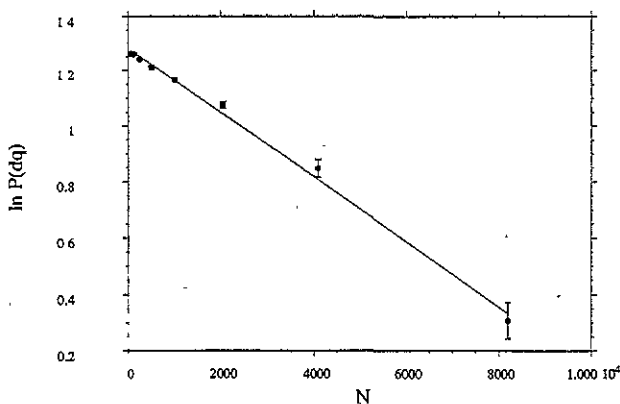


Figure 8. The same plot as in figure 7 for $\delta q = 0.125$.

values of δq , against $N \delta q^3$. This plot is very interesting because it shows that for each finite dimensionality a straight line gives a good fit to the data. Only for very large sizes would different straight lines superimpose on to the same line according to the scaling behaviour equation (38). These strong finite-dimensional corrections which violate the scaling behaviour equation (38) were already visible in figure 6. The interesting fact is that, even though we should expect a very large dimension in order to see the full scaling behaviour equation (38), the δq^3 behaviour in the scaling law (for a fixed size) survives down to small dimensionalities.

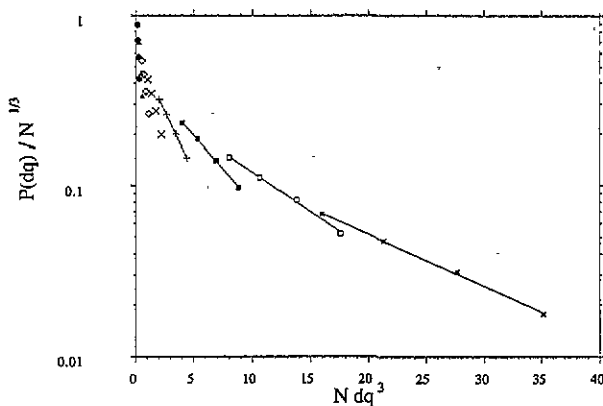


Figure 9. A test for the scaling behaviour equation (38) with the same parameters as in figures 7 and 8. For fixed size the $\exp(a\delta q^3)$ behaviour survives down to low dimensionalities. For very large sizes we hope all the lines will superimpose onto a unique one.

In summary, we observe that all our numerical results are in reasonable agreement with the theoretical predictions.

7. Conclusion

The nature of the finite-size corrections in the mean-field model of spin-glasses is a very interesting problem because it is the first step in understanding fluctuations within replica theory. Up to now, the critical point and the AT line have been well understood. Within the spin-glass phase the difficulty increases considerably. Only some partial results have been obtained in this case.

We have obtained the analytic formulae for the finite-size corrections to the moments of the distribution of overlaps $P(q)$ and of the distribution $\tilde{P}(\delta q)$ which describes the violation of the ultrametricity. In case of $P(q)$, the δ -function acquires a finite width, which is accessible to numerical simulation, and its square scales like $N^{-2/3}$. Furthermore we have calculated several quantities at the AT line, using a particularly simple form for the propagators. Among them we have discussed free energy and the internal energy both near and far from T_c .

All our predictions seem to be in good agreement with Monte Carlo simulations on the SK model. Finite-size corrections to the ultrametricity were simulated in the hypercube model. We investigated the possibility of a scaling law similar to that found for the distribution of overlaps $P(q)$. We have found that this scaling behaviour has strong finite-dimensional corrections. This was also observed for the second moment of the distribution $\tilde{P}(\delta q)$. Except for strong finite-dimensional corrections, the results seem to converge to the expected behaviour for high dimensionalities.

These results increase our knowledge of the mean-field theory of spin glasses. Some results have been obtained within the spin-glass phase. The question about the finite-size corrections for the free and internal energy within the spin-glass phase are open problems. In this case, the enormous difficulty which the full propagators presents makes progress slow. Nevertheless some results have already been obtained and will be presented in a forthcoming work.

Acknowledgments

We are grateful to I Kondor and T Temesvári for many stimulating discussions. FS also wishes to thank the APE group at Rome University for their kind hospitality. FR acknowledges the support of a grant from the European Community within the Science programme.

References

- [1] Edwards S F and Anderson P W 1975 *J. Phys. F: Met. Phys.* **5** 89
- [2] Kirkpatrick S and Sherrington D 1978 *Phys. Rev. B* **17** 4384
- [3] Parisi G 1980 *J. Phys. A: Math. Gen.* **13** L115, 1101, 1887
- [4] Mézard M, Parisi G, Sourlas N, Toulouse G and Virasoro M 1984 *J. Physique* **45** 843
- [5] Mézard M and Virasoro M 1985 *J. Physique* **46** 1293
- [6] De Dominicis C and Kondor I 1983 *Phys. Rev. B* **27** 606
- [7] Fisher D S and Huse D 1988 *Phys. Rev. B* **38** 386
- [8] De Dominicis C, Kondor I and Temesvári T 1991 *J. Phys. A: Math. Gen.* **24** L301
- [9] De Dominicis C and Kondor I 1985 *J. Physique Lett.* **46** L-1037
- [10] De Dominicis C and Kondor I 1985 *Lecture Notes in Physics* vol 216, ed L Garrido (Berlin: Springer) p 91
- [11] De Dominicis C and Kondor I 1984 *J. Physique Lett.* **45** L-205
- [12] Temesvári T, Kondor I and De Dominicis C 1988 *J. Phys. A: Math. Gen.* **21** L1145

- [13] Bhatt R N and Young A P 1986 *J. Magn. Magn. Mater.* **54-57** 191
Young A P 1983 *Phys. Rev. Lett.* **51** 1206
Reger J D, Bhatt R N and Young A P 1990 *Phys. Rev. Lett.* **64** 1859
Caracciolo S, Parisi G, Patarnello S and Sourlas N 1990 *Europhys. Lett.* **11** 783
- [14] Palmer R G and Pond C M 1979 *J. Phys. F: Met. Phys.* **9** 1451
- [15] Young A P and Kirkpatrick S 1982 *Phys. Rev. B* **25** 440
- [16] Parisi G, Ritort F and Rubí J M 1991 *J. Phys. A: Math. Gen.* **24** 5307
- [17] Parisi G, Ritort F and Slanina F 1993 *J. Phys. A: Math. Gen.* **26** 247
- [18] Bray A J and Moore M A 1978 *Phys. Rev. Lett.* **41** 1068
- [19] de Almeida J R L and Thouless D J 1978 *J. Phys. A: Math. Gen.* **11** 129
- [20] Franz S, Parisi G and Virasoro M A 1992 *J. Phys. I* **2** 1869
- [21] Franz S, Parisi G and Virasoro M A (in preparation)
- [22] De Dominicis C, Kondor I, Parisi G, Ritort F, Slanina F and Temesvári T to be published
- [23] Parisi G 1992 *Physica A* **185** 316